SOIL ECOLOGY LETTERS

SEL RESEARCH ARTICLE
Volume 8 / Issue 3 / 260409 / 2026
https://doi.org/10.1007/s42832-026-0409-4

Soil salinity alters acemannan content and sodium uptake in *Aloe barbadensis* Miller plants. A role for root-associated microbial communities?

Christina N. Nikolaou, Myrto Tsiknia*, Dionisios Gasparatos, Constantinos Ehaliotis*

Laboratory of Soil Science and Agricultural Chemistry, Department of Natural Resources and Agricultural Engineering, Agricultural University of Athens, Iera Odos 75, Athens, Greece
* Corresponding authors. E-mail: mtsiknia@aua.gr (M. Tsiknia); ehaliotis@aua.gr (C. Ehaliotis)
Received May 2, 2025; Revised January 4, 2026; Accepted January 7, 2026

© The Author(s) 2026. This article is published with open access at link.springer.com and journal.hep.com.cn

ABSTRACT

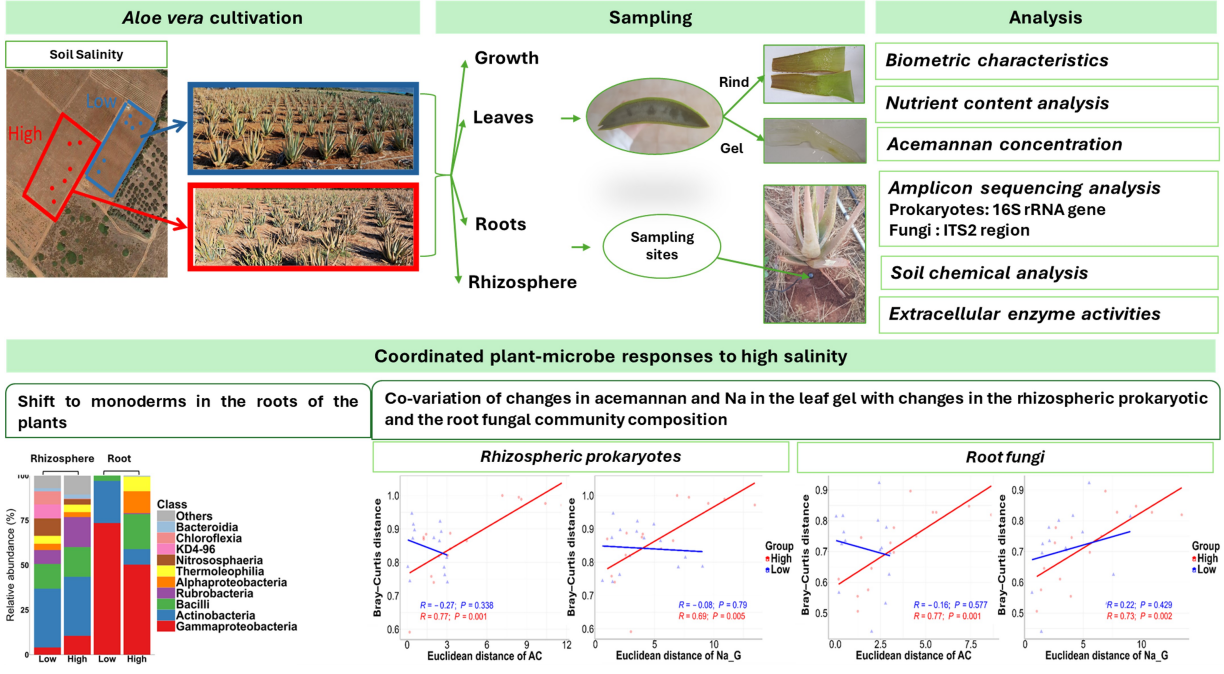

- Correlated acemannan and Na accumulation in leaf gel in response to soil salinity.
- Altered root-associated prokaryotic and fungal communities.
- Root prokaryotes shifted to monoderm bacteria associated with stress tolerance.
- *Aloe barbadensis* displays coordinated plant–microbe responses under soil salinity.

Salinity adversely impacts soil ecosystems, by inducing osmotic stress, ionic imbalances, water deficit, and oxidative damage in plants. It also alters the composition of plant-associated microbial communities in the rhizosphere and roots, while disrupting microbial processes critical to nutrient cycles. *Aloe vera* (*Aloe barbadensis* Miller), a xerophytic succulent plant, produces acemannan, a bioactive polysaccharide in its leaf gel with pharmaceutical applications. Acemannan contributes to drought tolerance by facilitating water storage within the leaf gel tissue. This study examined the effects of soil salinity on rhizosphere properties, plant nutrient acquisition, acemannan accumulation, and plant-associated microbial communities in *A. vera* plants grown in the field in Laconia, Greece. Both acemannan and sodium (Na) accumulated in the leaf gel in response to soil salinity, showing a strong positive correlation. Significant differences in the composition and structure of the rhizosphere and root microbial communities were also observed under salinity, with the prokaryotic microbial community in the plant roots showing a pronounced shift towards functionally relevant membership and abundance of monoderms. Moreover, we observed significant co-variation of changes in the acemannan

and Na concentrations in the leaf gel with changes in the prokaryotic rhizosphere soil community and the fungal community in the roots. Our findings demonstrate enhanced accemanan production and indicate links between osmolyte accumulation and microbial community adaptation in *A. vera* under soil salinity.

Keywords soil salinity, microbial communities, *Aloe vera*, acemannan

1 Introduction

Soil salinity presents major challenges to plant growth, soil fertility and productivity, and ecological stability worldwide (Zhou et al., 2017; Litalien and Zeeb, 2020; Jaiswal et al., 2022). Salinity induces ion availability changes and osmotic stress in the rhizosphere triggering substantial modifications in physiological and biochemical processes *in planta* (Zhou et al., 2024). Common effects include reduced photosynthesis and growth, oxidative stresses, and disruptions in nutrient uptake and homeostasis. However, plants differ widely in their sensitivity and adaptive responses to salinity (Roussos et al., 2013; van Zelm et al., 2020; Zhou et al., 2024).

At the same time, it influences the composition, structure and functions of soil microbial communities (Rietz and Haynes, 2003; Rath and Rousk, 2015; Philippot et al., 2021, 2024). Elevated salinity typically leads to reduced microbial biomass, microbial enzyme activities, and decomposition rates of organic matter (Singh, 2016; Boyrahmadi and Raiesi, 2018; Xu et al., 2021), though threshold values vary and are context dependent. Previous studies have reported that salinity reduces the activity of extracellular enzymes, such as *β*-glucosidase, urease, and phosphatase, which are critical for carbon, nitrogen, and phosphorus cycling (Wichern et al., 2006; Morrissey et al., 2014). The effects of salinity on the composition and structure of soil microbial communities, have been related to differences in tolerance of taxa and specific genotypes to osmotic stress and ion toxicity (Pankhurst et al., 2001; Nelson and Mele, 2007; Chowdhury et al., 2011). These shifts often reflect selection for functionally relevant traits resulting in microbial assemblages that exhibit greater salinity tolerance and ecosystem-level adaptation (Xu et al., 2021). Microbial community changes are particularly dynamic in the rhizospheric soil, where interactions with plant roots may play a major role in shaping the resilience and productivity of plant ecosystems under salinity (Yuan et al., 2016). However, while the impacts of salinity on soil properties, enzyme activities, and microbial communities are becoming increasingly well-documented, integrative studies linking these changes to plant secondary metabolism remain scarce.

Aloe vera is a xerophytic succulent belonging to the Asphodelaceae family and is widely valued for its nutraceutical and medicinal properties (Jales et al., 2021). Cultivated in arid and semi-arid regions, it has developed strategies to cope with osmotic stress caused by salinity and/or water scarcity (Quezada et al., 2017). The leaves are characterized by the formation of mucilaginous gel tissue between the abaxial and adaxial regions, known as the hydrenchyma, which functions mainly in water and energy storage (Salinas et al., 2019; Comas-Serra et al., 2024). Under osmotic stress, the gel plays a key role in maintaining tissue hydration by supporting osmotic adjustment processes within the leaf. Increases in water-soluble polysaccharides in the gel contribute to improved water retention and sustained photosynthetic activity in the chlorenchyma (Ahl et al., 2019; Fradera-Soler et al., 2022).

β-(1→4) acetylated glucomannan, commonly known as acemannan is one of the most important polysaccharides in *Aloe vera* leaf gel, exhibiting diverse pharmaceutical properties, including anti-cancer, anti-inflammatory, anti-diabetic and wound-healing activities (Choi et al., 2001; Bai et al., 2023; Nikolaou et al., 2023). Acemannan functions as an osmolyte, contributing to osmotic adjustment and water redistribution from the hydrenchyma to the chlorenchyma (Ahl et al., 2019; Salinas et al., 2019; Fradera-Soler et al., 2022). Its hydrophilic and acetylated structure also facilitates water sequestration within the hydrenchyma (Femenia et al., 1999; Fradera-Soler et al., 2022). Accordingly, acemannan levels are known to increase under drought stress (Salinas et al., 2019), and under combined drought and salinity stress (González-Delgado et al., 2023; Comas-Serra et al., 2024). However, no specific mechanism has been described for the accumulation of acemannan under salinity stress alone. This increase appears to arise from shared physiological responses under drought and salinity, as both are primarily manifested as osmotic stress (Wang et al., 2003). Supporting this, abscisic acid (ABA), a key hormone mediating plant tolerance to both salt and water stress, has been shown to induce acemannan synthesis in *Aloe vera* (Salinas et al., 2019).

In our study, we investigated the effects of soil salinity on the soil-microbiome-plant continuum. Specifically, we examined soil physicochemical properties, extracellular soil enzyme activities (EEAs), structure and function of rhizosphere and root-associated microbial communities, nutrient acquisition, and the compartmentalization of acemannan and sodium in *Aloe vera* leaves. Given acemannan's dual role as a valuable secondary metabolite and potential osmotic stress response compound, we specifically

examined how soil salinity influences acemannan accumulation in field-grown *Aloe vera*, and whether these changes are associated with shifts in root-associated microbial communities. The research was conducted in an organically cultivated field of 3 years old *Aloe vera* plants, in a coastal region in Laconia, Greece, where natural spatial variation in salinity was associated with distance from the coastline. We hypothesized that spatial variation in soil salinity within an otherwise homogeneous field would be associated with differences in: (i) the structure and composition of root-associated microbial communities, and (ii) plant physiological responses, including acemannan accumulation and nutrient partitioning.

2 Materials and methods

2.1 Experimental setup

This study employed an observational field survey design comparing two naturally occurring salinity zones within the same field. While this approach limits causal inference compared to controlled experiments, it allowed us to investigate plant–microbe–soil associations under authentic field conditions with shared pedoclimatic history and management practices. The study was conducted in an experimental organic *Aloe vera* farm, with a planting distance of 80 cm × 80 cm and a plantation density of 10 000 plants ha^{-1} located in the coastal region of Viglafia, Greece. All plants belonged to the same *Aloe vera* cultivar and originated from vegetative propagation through suckers derived from mother plants cultivated on-site. The region is characterized by a typical Mediterranean climate with a xeric soil moisture and a thermic soil temperature regime (latitude: 36.540, longitude: 23.025). Sampling was conducted in June 2022 to coincide with the period of elevated temperatures, during which *Aloe vera* exhibits enhanced secondary metabolic activity, including increased production of bioactive compounds. The field exhibited a naturally formed soil salinity gradient relevant to the distance from the coastline. Prior to sampling, soil electrical conductivity (EC) was measured *in situ* using a portable conductivity meter (averages of six replicates per area). We identified two areas with distinct soil salinity levels ("low" and "high") with mean bulk soil EC values of 0.8 dS m^{-1} in the low-salinity area and 2.1 dS m^{-1} in the high-salinity area, both planted with 3-year-old plants grown under the same cultivation protocols, that exhibited similar phenotypic characteristics across both areas. All plants were irrigated under the same drip irrigation regime during the growing season (spring–summer), typically 2–3 times per week depending on climatic conditions, ensuring uniform water input across both salinity zones. From each area, six plants were selected (biological replicates) and rhizospheric soil samples, leaves and roots (one leaf and root sample per plant) were collected, resulting in twelve in total samples for each plant compartment (rhizospheric soil, root, leaf), six from the low salinity area and six from the high salinity area. Plant biometric characteristics, including plant height, number of leaves, and number of offshoots, were measured in the field.

Rhizospheric soil samples consisted of three homogenized subsamples per plant collected from the proximal rhizosphere zone using a 5 cm diameter step-probe to a depth of 10 cm (Fig. S1). Root fragments were carefully removed and homogenized, while rhizospheric samples were sieved to 4 mm, and partitioned into a small part that was kept at –20 °C for DNA extraction and determination of extracellular soil enzyme activities (EEAs) (approximately 50 g) and to a larger part that was air dried and used for determination of soil physicochemical analysis (approximately 300 g). Immediately after sampling, root fragments were surface-sterilized by a single immersion in 1% (w/v) NaClO for 1 minute, followed by six rinses in sterile distilled water to remove residual disinfectant. Sterilized roots were then stored at –20 °C for DNA extraction. The leaves were separated into their outer rind and inner gel tissues. The rind samples were dried at 60 °C for nutrient content analysis. The gel samples were kept at –20 °C until they were lyophilized, for the determination of acemmanan and nutrient concentration analysis.

2.2 Soil physicochemical analysis

The electrical conductivity of the saturation paste extract (ECe) was measured for all soil samples (Carter, 1993). The saturation paste extract was also used to quantify the concentration of soluble cations Na, Ca, and Mg and to calculate the Sodium Absorption Ratio (SAR) index (Carter, 1993; FAO, 2020). Soil texture was estimated with the hydrometer method (Ashworth et al., 2001; FAO, 2020). The pH was measured using a standard glass/calomel electrode in 1:2.5 (w/v) ratio soil–$CaCl_2$ (0.01 M) suspensions (Carter, 1993). For the quantification of soil organic carbon content the potassium-dichromate oxidation method was used (Nelson and Sommers, 1996). The available P-olsen was estimated in sodium bicarbonate extracts, followed by the Murphy-Riley color reaction with a T60 UV/Vis spectrophotometer (PG instruments, United Kingdom), at 880 nm wavelength. Exchangeable cations (Na, K, Ca, Mg) and extractable Zn, Fe, and Mn were determined following the ammonium acetate (Carter, 1993) and diethylenetriaminepentaacetic acid (DTPA) extraction methods (Lindsay and Norvell, 1978), respectively.

2.3 Extracellular enzyme activity assays

The potential activities of five hydrolytic enzymes related to

C, N and P cycling were estimated, including *β*-galactosidases and *β*-glucosidases (breakdown of low molecular-weight carbohydrates), N acetylglucosaminidases (NAGase) (hydrolysis of chitin and peptidoglycan), alkaline and acid phosphatases (hydrolysis of organophosphates) (Tabatabai, 1994; Sinsabaugh et al., 2008; Jian et al., 2016).

The activities were measured by quantifying *p*-nitrophenol released from the substrates: pNP-*β*-glucopyranoside (for *β*-glusosidase, acetate buffer pH = 6), 4-nitrophenyl-*β*-D-galactopyranoside (for *β*-galactosidase, acetate buffer pH = 6), p-nitrophenyl-N-acetyl-*β*-D-glucosaminide (for NaGase, acetate buffer pH = 5.5), p-NP phosphate (for acid phosphatase, acetate buffer pH = 5). For alkaline phosphatase the incubation was carried out in tris acetate buffer pH = 8 (Tabatabai, 1994; Parham and Deng, 2000; Sun et al., 2017). The assays were performed in a microplate format according to Jackson et al. (2013) and soil slurries (2 g of soil added to 10 mL of buffer) were incubated with each substrate at 37 °C for 2 h (Tabatabai, 1994). *P*-nitrophenol (PNP) absorbance was measured at 410 nm wavelength using a Multiscan-Sky Microplate Reader (Thermo-Scientific). All enzymatic activities were assayed in triplicate and were expressed in μmol PNP h^{-1} g^{-1} dry soil.

2.4 Nutrients in leaf rinds and gel

The dried leaf rinds and lyophilized gels samples were finely ground in a stainless-steel Wiley mill. A subsample of 0.5 g for rinds and 50 mg for gels was heated to ash at 550 °C (Zheljazkov and Warman, 2002). The rind extracts were digested with 5 mL of 65% HNO_3, diluted to 25 mL with dH_2O and filtered. Similarly, gel extracts were digested with 1 mL of 65% HNO_3 and diluted to 10 mL with dH_2O. Total concentration of P was determined following the Murphy-Riley color reaction method, with a PG T60 UV/Vis spectrophotometer, at 880 nm wavelength (Olsen, 1954). K and Na were measured by flame photometry (PG 2000 Instruments). The concentrations of Mg, Fe, Zn and Mn were determined by flame atomic absorption spectrophotometry (Varian, A–300; Varian Techtron Pty. Limited, Mulgrave, Australia), using an air–acetylene flame, while Ca concentration was determined using an acetylene–N_2O flame. The N concentration in the rind samples was estimated in 0.5 g subsamples with the Kjeldahl method (Bremner, 1965).

2.5 Acemannan quantification assay

The acemannan content of gel samples was estimated using the spectrophotometric Congo Red method, (Eberendu et al., 2005; Cardarelli et al., 2013; Nikolaou et al., 2023), with certain modifications. Briefly, 10 mg of lyophilized gel was diluted to 50 mL of dH_2O after two hours of shaking at 28 °C and 30 min in an ultrasonic bath. The extract was passed through a 0.45 μm filter, before performing the color reaction. Konjac glucomannan (Megazyme) was used as standard (Quezada et al., 2017) and the absorbance was measured at 540 nm using a T60 UV/Vis spectrophotometer (PG instruments, United Kingdom).

2.6 Amplicon sequencing and bioinformatic analysis

DNA extraction from each soil sample (0.25 g) was performed with the DNeasy Power soil DNA isolation kit (Qiagen, Hilden, Germany) and from root samples with the NucleoSpin Plant II kit (MACHEREY-NAGEL, Germany) following the manufacturer's instructions. The amplification of the bacterial and archaeal 16S rRNA genes was performed with the primer set 515f–806r (Caporaso et al., 2012; Walters et al., 2016), which targets the V4 region of the 16S rRNA, following the protocol of the Earth Microbiome Project (Caporaso et al., 2018). The fungal ITS region was amplified using the primers ITS7f—ITS4r (White et al., 1996; Ihrmark et al., 2012), following the protocol described by Ihrmark et al. (2012). A two-step PCR was conducted using the Q5® High—Fidelity DNA Polymerase (NEB, Ipswich, Massachusetts, USA). During the second PCR, for each gene region, a unique 12-bp index was added to serve as a barcode to identify each sample in the multiplexed libraries based on in-house protocols (Vasileiadis et al., 2015, 2018). Amplicons were sequenced *via* MiSeq Illumina v3 2×300 bp paired end reads at the Greek Genome Center of the Biomedical Research Foundation Academy of Athens (BRFAA, Athens, Greece). Flexbar v3.0 (Dodt et al., 2012) was used to de-multiplex by sample the retrieved reads. The de-multiplexed paired end sequences were then clustered into amplicon sequence variants (ASVs) after processing with the DADA2 package (Callahan et al., 2016), following the standard operation procedure. Taxonomic information was assigned to ASVs based on Silva v138.1 small ribosomal subunit database (Yilmaz et al., 2014) for prokaryotes and on UNITE database v9.0 (Nilsson et al., 2019) for fungal community.

A total of 494 361 and 655 951 paired-end sequence reads were obtained and assembled for the prokaryotic and fungal community, respectively. After further processing for removing low quality reads and chimeras 163 736 and 219 807 reads remained for the 16S and ITS region, respectively. Non-target taxa (e.g., NAs at Kingdom level, chloroplasts and mitochondria for the 16S rRNA gene and unknown or protists for the ITS) and ASVs with relative abundance <0.1% were excluded. Finally, 364 prokaryotic and 360 fungal ASVs were included in downstream analysis.

2.7 Statistical analysis

All statistical analyses were conducted using the R

software (v.4.3.1) (R Core Team et al., 2022). Independent (Two-Sample) Student's *t*-Test was performed to assess whether rhizospheric soil and plant sampling properties differed significantly between the two salinity areas. All values are presented as the mean ± standard error of mean. Possible correlations among acemannan concentration, EEAs and plant/soil variables were assessed using Spearman's rank correlation coefficient (r_s). *p*-values were adjusted using the Benjamini–Hochberg false discovery rate (FDR) procedure.

Differences in prokaryotic and fungal rhizospheric and root microbial composition, structure and *α*- and *β*-diversity patterns were analysed/compared across the two salinity areas. *α*-diversity metrics, Observed ASVs and Shannon diversity were computed with *vegan* package (Dixon, 2003). *β*-diversity patterns were visualized by Principal Coordinate Analysis (PCoA) based on the Bray–Curtis dissimilarity metric and PERMANOVA was conducted with 999 permutations in *microeco* package (Liu et al., 2021). Relative abundances for both prokaryotes and fungi were calculated and visualized using the *microeco* package. Differentially abundant ASVs (bacterial and fungal) that varied significantly in abundance between the two salinity levels in the rhizosphere and in the root community were identified with the Kruskal–Wallis and the Wilcoxon rank-sum post-hoc tests, as employed by Bekris et al. (2021) to the top 200 more abundant ASVs. To investigate potentially significant correlations between prokaryotic/fungal *β*-diversity patterns and plant/soil variables the Mantel test was performed (according to Pearson correlation (R), using 999 permutations), for each salinity driven habitat variant, between Bray–Curtis distances of community composition and Euclidean distances of plant/soil variables, using the *microeco* and *vegan* package. All plots were created in R with the packages *microeco*, *ggplot2* (Wickham, 2016) and *ggpubr* (Kassambara, 2023).

3 Results

3.1 Rhizosphere soil properties

Data on rhizospheric soil properties are summarized in Table 1. The soil was a loamy sand and exhibited three-fold higher electrical conductivity (ECe) in the rhizosphere samples of the high salinity area, reaching 10.7 ± 0.8 dS m^{-1},

Table 1 Rhizosheric soil properties of the low vs high salinity area.

Rhizospheric soilproperties	Salinity level		*t*-Test
	Low	High	
Silt (%)	13.0 ± 0.05	10.0 ± 0.7	ns
Clay (%)	12.0 ± 0.4	13.0 ± 0.1	ns
Sand (%)	75.0 ± 0.08	77.0 ± 0.4	ns
ECe (dS m^{-1})	3.3 ± 0.7	**10.7 ± 0.8**	**
SAR	5.5 ± 0.2	**12.1 ± 0.1**	***
pH (1:2.5 (w/v) in $CaCl_2$ (0.01M))	**7.1 ± 0.05**	6.7 ± 0.04	**
Na-Exch (mg kg^{-1})	340 ± 71.4	**1,040 ± 178**	**
K-Exch (mg kg^{-1})	238 ± 32.2	201 ± 20.8	ns
Ca-Exch (mg kg^{-1})	1,426 ± 179	1,121 ± 164	ns
Mg-Exch (mg kg^{-1})	260.0 ± 23.3	302.6 ± 28.4	ns
Fe-DTPA (mg kg^{-1})	5.0 ± 0.4	**9.0 ± 1.0**	*
Zn-DTPA (mg kg^{-1})	1.5 ± 0.1	**2.7 ± 0.4**	*
Mn-DTPA (mg kg^{-1})	3.0 ± 0.4	3.3 ± 0.7	ns
P-Olsen (mg kg^{-1})	5.9 ± 0.5	**21.3 ± 3.2**	**
SOC (%)	0.55 ± 0.04	0.50 ± 0.04	ns
β-Glucosidase (μmol PNP g^{-1} soil h^{-1})	1.1 ± 0.2	1.0 ± 0.02	ns
β-Galactosidase (μmol PNP g^{-1} soil h^{-1})	0.26 ± 0.02	0.20 ± 0.03	ns
NaGase (μmol PNP g^{-1} soil h^{-1})	0.39 ± 0.07	0.28 ± 0.09	ns
Acid phosphatase (μmol PNP g^{-1} soil h^{-1})	1.9 ± 0.2	1.8 ± 0.3	ns
Alkaline phosphatase (μmol PNP g^{-1} soil h^{-1})	0.50 ± 0.1	**1.5 ± 0.2**	*

Average values are presented ± standard errors (n = 6). Significance is indicated with * for $p < 0.05$, ** for $p < 0.01$, *** for $p < 0.001$. ns, non-significant, based on *t*-Tests. Abbreviations: ECe, electrical conductivity of the saturation paste extract; SAR, sodium adsorption ratio; SOC, soil organic carbon; Exch, exchangeable; NaGase, N-acetyl-β-glucosaminidase; PNP, p-nitrophenol.

compared to those of the low salinity area ($p < 0.01$). Exchangeable Na and P-Olsen values were also three-fold higher in the high salinity area reaching 1040 and 21.3 mg kg^{-1} respectively ($p < 0.01$), while the Sodium Absorption Ratio (SAR) doubled reaching 12.1 ($p < 0.001$). Regarding micro-nutrients, Fe-DTPA and Zn-DTPA were higher (nearly double) in the high salinity area ($p < 0.05$). On the contrary, the pH was slightly, but significantly, lower in the high salinity area (6.7), compared to the low salinity area (7.1, $p < 0.01$). All other soil properties including macro- and micro-nutrients and organic matter content presented similar values in the two salinity areas (Table 1).

The potential enzyme activity profiles were not affected by soil salinity, with the notable exception of the alkaline phosphate which was increased three-fold in the rhizosphere soil under high salinity ($p < 0.05$, Table 1). β-glucosidase, showed a negative correlation with ECe in the rhizosphere soil in the high salinity area ($r_s = -0.906$, $p < 0.05$) and with soil Na availability in the low salinity area ($r_s = -0.924$, $p < 0.05$).

3.2 Plant growth and concentrations of acemannan and nutrients in the leaves

Plants did not differ in their main biometric growth characteristics (height, number of leaves and offshoots) between the high and low salinity areas (Table S1). However, plants cultivated in the high salinity area demonstrated significantly higher accumulation of acemannan ($p < 0.01$) (Fig. 1) compared to those grown under low salinity conditions. The leaf rinds of the plants grown under high salinity exhibited significantly higher Fe ($p < 0.05$) concentrations but lower K ($p < 0.05$) (Table 2), while their gel showed significantly higher concentrations of Na ($p < 0.01$) and P ($p < 0.01$) but lower K ($p < 0.05$) and Mg ($p < 0.001$) (Table 2). Acemannan concentration was positively correlated with the concentration of Na ($r_s = 0.96$, $p < 0.01$) and Fe ($r_s = 0.88$, $p < 0.05$) in the leaf gel, and with P ($r_s = 0.85$, $p < 0.05$) in the leaf rinds of the plants grown under high salinity, but not of those under low salinity (Spearman rank correlation tests, Table S2).

3.3 The effect of salinity on microbial community composition

Prokaryotic and fungal communities tended to show greater richness and diversity in the rhizospheric soil compared to the root environment (Figs. S2, S3), but these differences were not statistically significant. Salinity had no effect on the α-diversity indexes of prokaryotes, apart from leading to more consistent diversity values in the roots (Fig. S2). For the fungal communities, salinity led to lower richness and diversity in the rhizospheric soil, but to increased values for both indexes in the roots (Fig. S3).

Regarding β-diversity, PERMANOVA test based on the Bray–Curtis dissimilarity metric showed that salinity had a

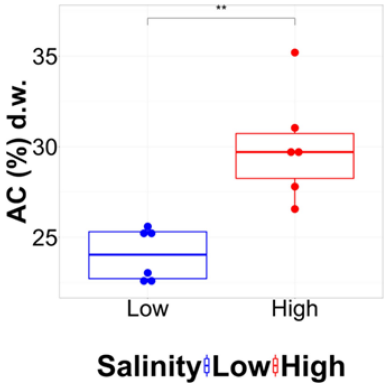

Fig. 1 Content of acemannan (AC% d.w.) in the leaf gel of *Aloe vera* plants grown in the low vs. high salinity area. The upper and lower box boundaries indicate the 75th and the 25th percentiles, respectively; the midline indicates the median, and the whiskers above and below indicate the 90th and 10th percentiles, respectively; the dots indicate outliers ($n = 6$). Significance is indicated with * for $p < 0.05$, ** for $p < 0.01$, *** for $p < 0.001$, based on *t*-Tests.

Table 2 Concentration of the minerals in the leaf rind and gel of *Aloe vera* plants grown in the low vs high salinity area.

	Rind minerals		*t*-Test	Gel minerals		*t*-Test
	Low salinity	High salinity		Low salinity	High salinity	
N (%)	6.5 ± 0.3	7.5 ± 0.4	ns	-	-	
Na (g kg^{-1})	14.8 ± 1.0	15.3 ± 0.9	ns	25.4 ± 1.3	**34.7 ± 1.9**	**
K (g kg^{-1})	**8.7 ± 0.8**	5.3 ± 0.6	*	**10.1 ± 0.4**	6.6 ± 1.1	*
Na/K	1.7	2.9		2.5	5.3	
Ca (g kg^{-1})	10.3 ± 1.2	8.9 ± 1.3	ns	23.0 ± 4.3	17.0 ± 2.8	ns
Mg (g kg^{-1})	4.8 ± 0.4	4.6 ± 0.4	ns	**4.5 ± 0.1**	3.2 ± 0.1	***
P (g kg^{-1})	0.46 ± 0.04	0.55 ± 0.05	ns	0.30 ± 0.01	**0.40 ± 0.01**	**
Fe (mg kg^{-1})	53.3 ± 4.5	**74.5 ± 4.6**	*	85.9 ± 5.2	79.8 ± 11.2	ns
Zn (mg kg^{-1})	11.2 ± 0.8	11.6 ± 0.9	ns	30.4 ± 0.8	34.1 ± 4.3	ns

Average values are presented ± standard errors ($n = 6$). Significance is indicated with ns, non-significa; * $p < 0.05$; ** $p < 0.01$; *** $p < 0.001$; based on *t*-Tests.

significant effect on both the rhizospheric prokaryotic (p < 0.01) and fungal communities (p < 0.05), whereas in the roots, soil salinity significantly affected the prokaryotic (p < 0.05), but not the fungal community composition (p > 0.05) (Fig. 2). PCoA visualization also showed that both the prokaryotic and fungal communities diverged and clustered in distinct groups under low compared to high salinity, even for the fungal communities in the roots (Fig. 2). The strongest clustering into distinct groups under high and low salinity according to the PCoA, appears to occur in the rhizosphere for both prokaryotes and fungi.

3.4 Composition of Microbial Communities

The prokaryotic community composition in the rhizosphere differed substantially between salinity levels. Under high salinity, notable increases were observed in the relative abundance of *Actinobacteria* and *Rubrobacteria* (Fig. 3A), bacterial groups commonly enriched in arid and saline environments due to their osmotolerance and ability to form resistant spores or produce compatible solutes. Conversely, *γ*-Proteobacteria decreased in relative abundance under high salinity, consistent with their generally lower salt tolerance. These compositional shifts likely underline the *β*-diversity patterns observed in PERMANOVA (Fig. 2), where salinity explained 15% of community variation.

Within the root-associated communities, the most striking change was the appearance of several normally soil-dwelling lineages (including Chloroflexi class KD4-96 and certain Actinobacteria) under high salinity, which may explain the increased *α*-diversity in this compartment (Fig. S2). This pattern suggests that salinity stress may alter root physiology or exudation profiles in ways that permit colonization by a broader taxonomic spectrum of soil microorganisms.

At the ASV level, differential abundance analysis revealed enrichment of two Rubrobacteria ASVs, one *Candidatus Nitrososphaera*, one Planococcaceae, one Micrococcaceae and one KD4-96 (uncultured and unclassified class-level taxon within the phylum Chloroflexi (Quast et al., 2013; Parks et al., 2020) under low salinity. In contrast, high salinity was associated with enrichment of four members of Plano-

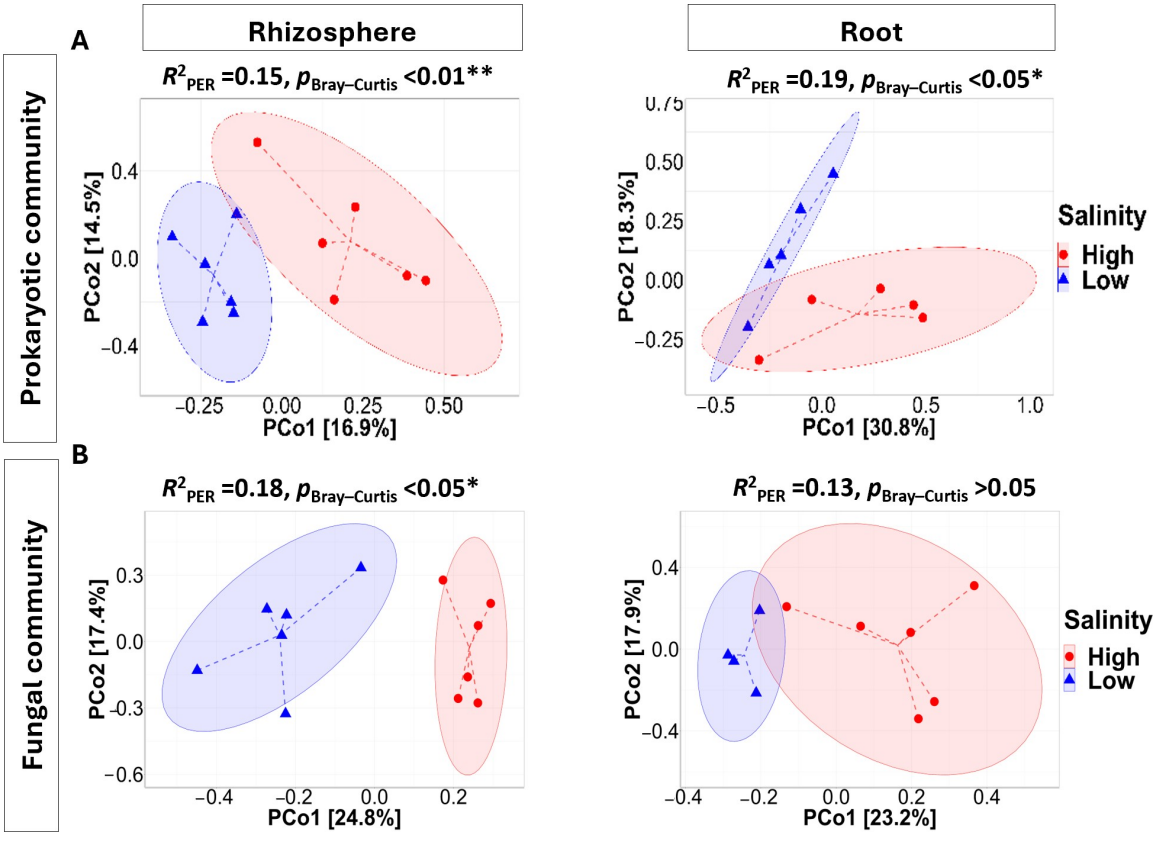

Fig. 2 Principal Coordinate Analysis (PCoA) based on Bray–Curtis dissimilarity metric for prokaryotic (A) and fungal (B) communities among two salinity levels of the rhizosphere and root. Each dot represents the corresponding community of a single sample (biological replicate). Lines connect the dots with the centroid of each grouping factor. Ellipses represent the 95% confidence interval around the group's centroid. The effect of salinity level according to PERMANOVA results based on Bray–Curtis dissimilarity metric is shown above each corresponding PCoA plot (***, **, and * indicate significance at $p_{Bray\text{-}Curtis}$ < 0.001, 0.01, and 0.05, respectively, based on 999 permutations and R^2_{PER}, the percentage of the total variation explained by salinity).

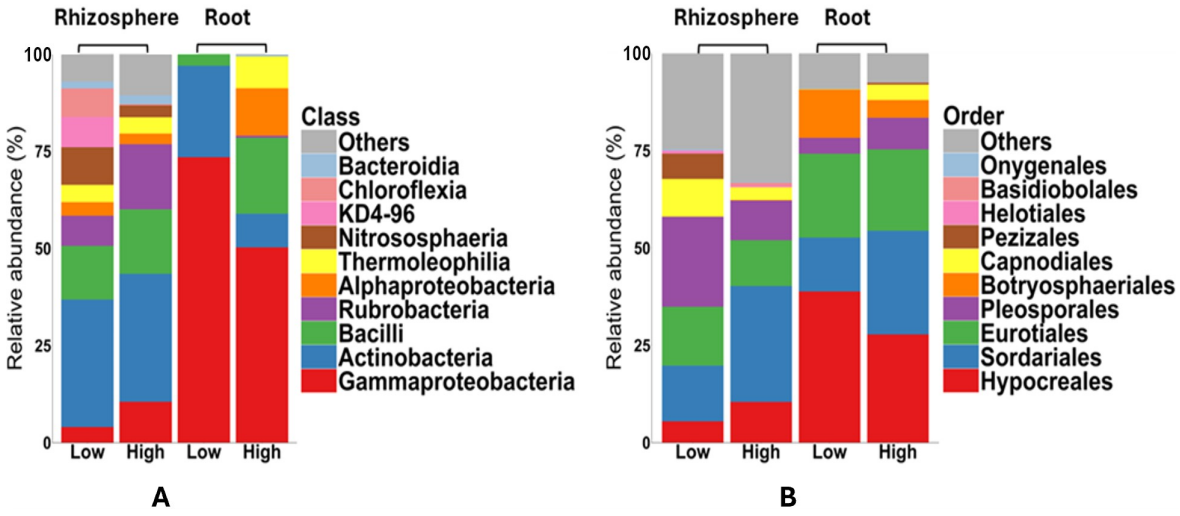

Fig. 3 Taxonomic composition of prokaryotic (A) and fungal communities (B), at the class and order level, respectively, across the two salinity areas for each examined habitat (rhizosphere and root).

coccaceae and one of Bacillaceae (all Firmicutes) and one Enterobacterales (gamma-Proteobacteria) (Fig. S4A). The root prokaryotic community of the plants grown under low salinity showed low richness at the Class level and was over-dominated by gamma-Proteobacteria, mainly Enterobacterales followed by Xanthomonadales and Pseudomonadales. Actinobacteria, mainly Streptomycetales were also prevalent, and *Bacilli* were present at lower abundances (Fig. S5). However, in the roots of the plants grown under high salinity Thermoleophilia and alpha-Proteobacteria were also prevalent, while Rubrobacteria and Bacteroidia were also present at low abundances, giving rise to a more diverse prokaryotic root community. For the root prokaryotic community, one ASV of Enterobacterales, one Streptomyces and two Rhodanobacteraceae were enriched under low salinity. In contrast, under high salinity only one ASV belonging to the Rhodanobacteraceae family was enriched (Fig. S4B).

The fungal community composition in all habitats and salinity levels was composed mainly by Ascomycota of the orders of Hypocreales, Sordariales, Pleosporales, Eurotiales, Capnodiales (Fig. 3B). However, in the rhizosphere of the low salinity area the order of Pezizales was also prevalent. At the ASV level, all enriched ASVs at low salinity, were affiliated with unidentified fungal taxa, but at high salinity one member of the Sordariomycetes (ASV23) and one of the Papulaspora (ASV 45), a Dark Septate Endophyte (DSE), were enriched (Fig. S4C). The fungal communities in the roots were dominated by three classes: Hypocreales, that showed increased abundance compared to the rhizosphere soil environment, Eurotiales, and Sordariales. In addition, Ascomycota of the order of Botryosphaeriales were represented in the roots of the plants grown in both high and low salinity. At the ASV level, no significant enrichment was detected in the root community under low salinity, but under high salinity we identified ASV23, that was also enriched in the rhizoshere and one member of the Papulaspora (ASV 72), a Dark Septate Endophyte (DSE) (Fig. S4D). Similarly to the prokaryotic communities, a wider range of fungal classes were observed in the roots under high salinity.

3.5 Relationships of microbial community composition with plant osmolytes

We tested for putative correlations of variations in soil properties, nutrient concentration and accumulation of osmolytes and acemannan (Euclidean distances) with bacterial/fungal community composition (Bray–Curtis dissimilarity distances), within each salinity area. Statistically significant associations under low and high salinity conditions for each microbial community are summarized in Tables S4 and S5 for prokaryotic and fungal communities respectively. Differentiations in the rhizospheric prokaryotic community composition were positively correlated with changes in acemannan (R = 0.77, P = 0.001) and Na concentration (R = 0.69, P < 0.01) in the leaf gel under high salinity (Fig. 4A and 4B). Similarly to the rhizospheric prokaryotic community, differentiations in the root fungal community composition were positively correlated with changes in acemannan (R = 0.77, P = 0.001) and Na concentration of the leaf gel (R = 0.73, P < 0.01) under high salinity (Fig. 4C and 4D). No significant correlations were observed for changes in the rhizosphere-fungal and the root-prokaryotic communities with changes in osmolytes *in planta* (Fig. S6).

4 Discussion

We focused on the spatial differentiation of soil salinity in an otherwise homogenous field cultivated organically with *Aloe*

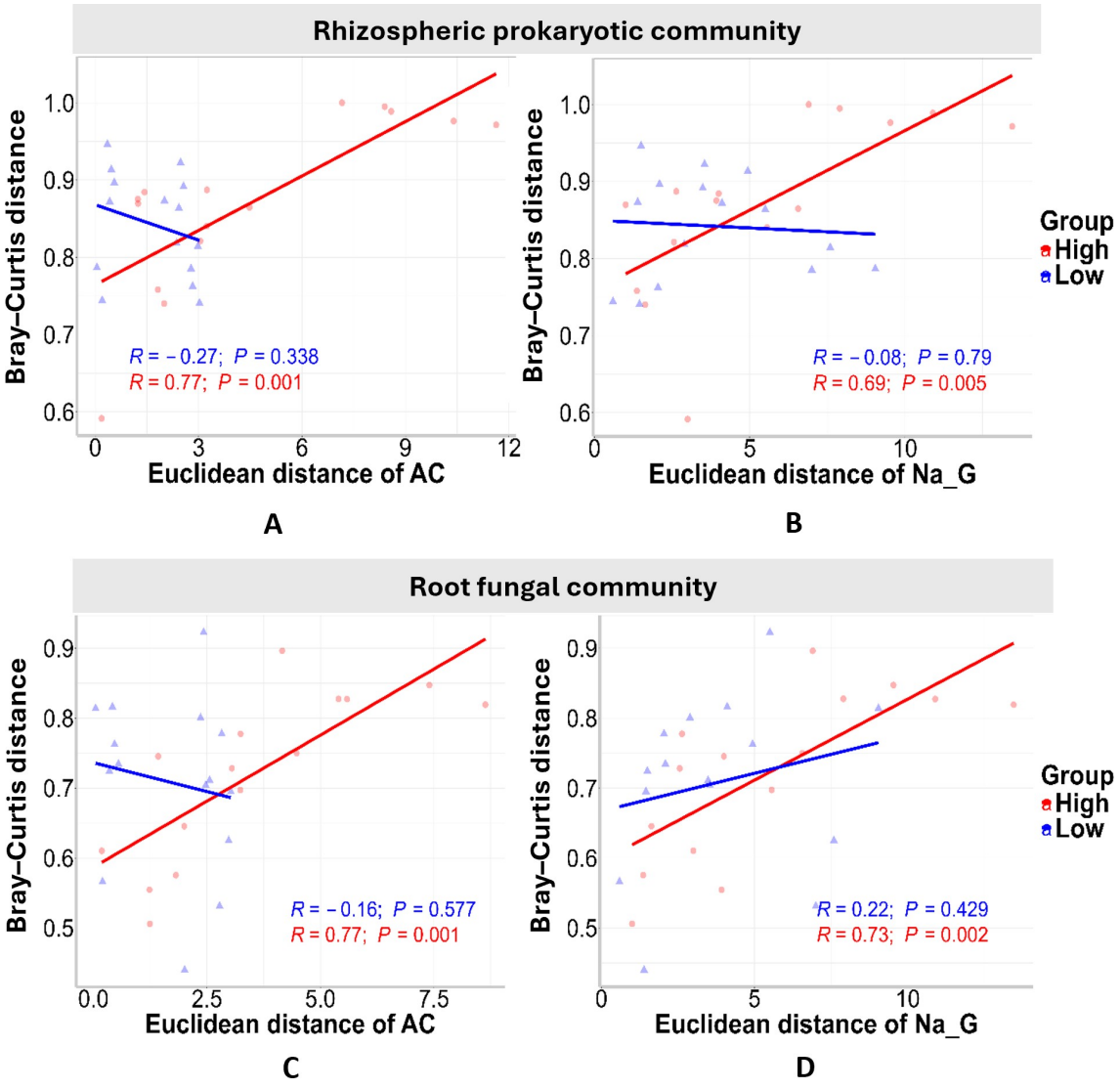

Fig. 4 Correlation analysis, performed using the Pearson R correlation coefficient, between the rhizospheric prokaryotic community or root fungal community Bray–Curtis distances with the Euclidean distances of plant variables (Acemannan and Na in leaf gel) for each salinity level. The scatterplots show linear correlation curves for Acemannan (AC) (Panels A/C) and Na in the leaf gel (Na_G) (Panels B/D). Values of R and P displayed in each panel correspond to the Pearson correlation coefficient and the associated *p*-value, respectively.

vera plants, to investigate the interplay between soil salinity, accumulation of acemannan polysaccharides *in planta*, and plant-associated microbial communities. Our observational design does not allow us to definitively isolate salinity effects from potential baseline differences in microbial communities or unmeasured soil properties. Future controlled experiments manipulating salinity levels with replicated randomized plots would complement these findings by establishing causal relationships. We hypothesized that elevated soil salinity would be associated with accumulation of acemannan in *A. vera* leaves. Accumulation of acemannan in the gel compartment of *A. vera* leaves may result as a response to osmotic stress induced by Na in the rhizosphere environment (González-Delgado et al., 2023; Comas-Serra et al., 2024). However, its relation to Na and K acquisition and allocation, and to shifts in root- and rhizosphere-associated prokaryotic and fungal microbial communities remains poorly understood.

4.1 Na, K and acemannan interplay

Plants exhibit specific mechanisms to tolerate salinity, including vacuolar compartmentalization of toxic anions, exclusion of Na ions, osmotic adjustments through the accumulation of compatible solutes and enhanced production of antioxidants (Shanker and Venkateswarlu, 2011; van Zelm et al., 2020; Ntanos et al., 2021). *A. vera* is a xerophytic plant with succulent leaves that exhibits crassulacean acid metabolism (CAM), which improves water-use efficiency by shifting CO_2 uptake to nighttime thereby reducing evaporative

water loss, while accumulating non-ionic osmoregulators under salinity stress (Derouiche et al., 2023). A three-fold higher concentration of exchangeable Na was observed in the rhizosphere soil in the high salinity area. Na in the leaves accumulated mainly in the leaf gel, where its concentration was significantly higher in the plants grown under high salinity compared to those grown under low salinity, but it remained low and showed no significant differentiation in the leaf rinds. This indicates activation of tolerance rather than Na exclusion mechanisms (Munns and Tester, 2008) by compartmentalization of excess Na taken up by the plants inside the leaf gel tissue and away from sites of metabolism, to bypass toxicity related to Na overaccumulation. Moreover, under high salinity, the Na-to-K ratios were over-doubled, from 2.5 to 5.3, in the leaf gel, but were only increased from I.7 to 2.9 in the leaf rinds (Table 1), thus protecting K^+ homeostasis (Assaha et al., 2017) and facilitating leaf physiological functionality in the rinds. Potassium ions are essential for metabolic functions occurring in the cytosol, but they also function as osmoregulators protecting succulent plants from salt stress. Besides, Na^+ uptake and its consequential influx into the cytoplasm causes membrane depolarization resulting in the extrusion of K^+ (Shabala and Pottosin, 2014). High soil K availability is therefore essential for protecting plants from Na-induced salinity stress. In our work, K availability in the rhizosphere soil of the *A. vera* plants (201–238 mg kg^{-1} soil) may be considered agronomically adequate, based on estimations for *A. vera* plants grown in a more acidic and heavy-texture soil (Sultana et al., 2021). However, K concentrations in the leaf rinds were comparatively low, indicating that K fertilization could further improve tolerance of Na-associated salinity in the *A. vera* plants. Genes coding for salt overly sensitive (SOS), vacuolar Na^+/H^+ antiporter (NHX) and sodium transporter (HKT1) proteins, involved in Na^+ recirculation/sequestration and K^+ transport selectivity (Ali et al., 2019) may also be involved in ion homeostasis and the observed resilience of the Na-to-K ratios in the leaf rinds under salinity, but specific experimentation is needed to examine their precise role.

Apart from Na, acemannan concentration was also higher in the leaf gel of plants grown under high salinity compared to those under low salinity. Acemannan functions as a non-toxic non-ionic compatible solute which *A. vera* plants accumulate to maintain osmotic balance and cellular function. Therefore acemannan accumulation may increase when the plants are exposed to drought or salinity stress (Salinas et al., 2019; González-Delgado et al., 2023). In our case study, since no phenotypic changes were observed (Table S1), Na compartmentalization and acemannan accumulation apparently functioned efficiently as adaptive responses of the plants to the high salinity in the root zone. Abscisic acid (ABA) levels increase dramatically *in planta* in response to salt or drought stress, leading to ABA-induced upregulation of a range of osmotic stress responsive genes (Dilukshi Fernando and Schroeder, 2016). Among these genes, the expression of the gene responsible for acemannan backbone synthesis, encoding a glucomannan mannosyltransferase (GMMT, EC 2.4.1.32) has indeed been shown to be induced in *A. vera* by ABA under drought stress (Salinas et al., 2019). Plants experience two-stage salinity stress: Initially osmotic stress occurs in the rhizosphere, calcium signaling is observed in the roots (Knight et al., 1997) and, following ion uptake, accumulation of both Na^+ and Cl^- ions progressively generates ionic stress *in planta* (Tester and Davenport, 2003; Munns and Tester, 2008). Therefore, we propose that the highly significant correlation of acemannan and Na, observed under high salinity in the leaf gel of *A. vera* is associated with two complementary processes. Acemannan accumulation in the leaf gel of *A. vera* is initiated upon osmotic stress involving ABA-induced upregulation of relevant genes, while Na accumulation in the leaf gel occurs at a later stage as a compartmentalization response to excess Na uptake. ABA, synthesized in roots in response to salinity, may also have a role in regulating K^+ channels (Roberts and Snowman, 2000; Deinlein et al., 2014), however targeted experimentation is needed to investigate this.

4.2 Salinity and plant tolerance—a link to root microbiomes

Salinity has been identified as an important factor in shaping the composition of microbial communities in soil (Wichern et al., 2006; Xu et al., 2021). In our work, PERMANOVA showed indeed that the composition of the prokaryotic and fungal communities differed significantly in the rhizosphere soil between high and low salinity. PERMANOVA also revealed significant dissimilarities in community composition of the prokaryotes in the roots of the *A. vera* plants, but not for the fungi. The partially shared root fungal microbiome may be attributed to the propagation strategy used in *Aloe vera* cultivation: The new plants derive from suckers formed on the mother plants that are already established in the field. As a result, the new plants are expected to sustain a great part of the microbiome of the mother plant, which was already partially shared before their establishment in the field (Nakkeeran et al., 2021).

Further, we focused on the qualitative and functional characteristics of the differences between microbiomes. The roots of the *A. vera* plants were inhabited by prokaryotes belonging to fewer major taxa compared to the rhizosphere, confirming that roots function as a strong selection filter for the prokaryotic rhizosphere microbiota (Bulgarelli et al., 2012). Gama-proteobacteria became the dominant class of prokaryotes within the roots (over 70% of the relative abundance of taxa, mainly from the Enterobacterales order, followed by Actinobacteria and the rare presence of Bacilli).

Previous studies have highighted that members of the Enterobacterales order, notably genera like Pantoea and Enterobacter, are frequently isolated from the roots of *Aloe vera* plants (Akinsanya et al., 2015; Nikolaou et al., 2023). These endophytic bacteria often possess a suite of plant growth-promoting (PGP) characteristics suggesting that these taxa may play a crucial role in the resilience of the *A. vera* plants in field. Remarkably though, the overdominance of Gammaproteobacteria was significantly reduced under high salinity and the taxonomic richness within the roots was greatly increased: major taxa, including Thermoleophilia, Alphaproteobacteria, Rubrobacteria and Bacteroidia reappeared among the root colonizers under high salinity, while Bacilli became a major taxon. This is consistent with a functionally pertinent modification, occurring in the roots but not in the rhizosphere, signifying the activation of root selection mechanisms under salinity: The overdominance of the Gram-negative Gamma-Proteobacteria was reduced and balanced mainly by a range of Gram-positive monoderms, including Bacilli, Actinobacteria (which maintain their high abundance), Thermoleophilia, Rubrobacteria and Bacteroidia. Preferential colonization of plant roots by Proteobacteria and other diderms, followed by a clear shift to monoderm bacterial colonizers under drought stress, has been convincingly presented as a mechanism of adaptation of plants to drought (Xu and Coleman-Derr, 2019; Breitkreuz et al., 2021). Plants appear to facilitate this shift by producing specific carbohydrate and amino-acid compounds under drought stress, which monoderm bacteria may specifically utilize, for example glycerol-3-phosphate (G3P) which is an important precursor to peptidoglycan biosynthesis and allows monoderm bacterial to build thick cel walls. ABC transporters of G3P are highly upregulated in monoderm bacteria while G3P has been shown to be produced by sorghum roots under drought stress (Xu et al., 2018). Moreover, monoderms have been shown to be less sensitive to reactive oxygen species (ROS) produced in the roots under drought stress compared to diderms (Mai-Prochnow et al., 2016). Here we show characteristic shifts from prokaryotic diderms towards monoderns in the roots of *A. vera* plants under high salinity. Furthermore, differential abundance analysis at the ASV level revealed that at rhizoshere, monoderm taxa mainly affiliated to the Firmicutes, where enriched under high sainity. We suggest that the respective overtripling of the electrical conductivity from 3.3 to 10.7 ds m^{-1}, and of Na from 340 to 1040 mg kg^{-1} in the rhizosphere soil induces strong osmotic stress, leading to plant root metabolic responses and relevant microbial community shifts analogous to shifts observed under drought.

Notably, the observed increase of the taxonomic richness within the roots under high salinity is also in accordance with the intermediate disturbance hypothesis (IDH), which predicts a maximum level of diversity at intermediate levels of disturbance or stress, due to trade-offs between species ability to cope with disturbance and their competitive ability (Grime, 1973; Connell, 1978) and has been shown to apply in soil microbial communities, leading to increased functional soil microbial diversity under adequate resource availability (Zhang et al., 2018).

Changes in the presence of high order fungal taxa within rhizosphere and root microbiomes were less dramatic compared to those for prokaryote taxa, in line with numerous observations regarding other plants under abiotic stress (Barnard et al., 2013; Furze et al., 2017; Santos-Medellín et al., 2017; Koyama et al., 2018). We may confirm, however, a consistent rise in the abundance of *Sordariomycetes* under salinity which have been reported to also prevail under high salinity in other soil environments (Chen et al., 2022; Zhang et al., 2023). Certain members of the *Papulaspora* genus, enriched in both the rhizosphere and root communities, are classified as dark septate endophytes (DSEs). These fungi are important players in enhancing plant nutrition through nutrient acquisition and in alleviating abiotic stresses like drought and salinity (Mandyam and Jumpponen, 2005). Regarding differences between the rhizosphere and the root fungal microbiomes the appearance of Botryosphaeriales and the higher abundance of Hypocreales in the roots was observed, both groups including well-known fungi with endophytic lifestyles.

Changes in extracellular enzyme activities under salinity indicate functional adaptations of the soil microbial communities. Generally, salinity is reported to have a negative impact on the potential activity of extracellular soil enzymes (Frankenberger and Bingham, 1982; Singh, 2016; Dong et al., 2022). Potential enzyme activities related to C cycling (beta-gucosidase, beta-galactosidase) and N cycling (N-acetyl-*β*-glucosaminidase) did not change significantly between normal and high salinity in the rhizosphere soil of our study area. However, the general trend for lower values in the high salinity area, and the negative correlation of beta-glucosidase with soil ECe in the high salinity area, and with soil Na availability in the low salinity area indicate partial suppression. Microbial adaptation to salinity or to substrate availability in the form of root deposition and exudates under salinity in the rhizosphere may have partly counterbalanced osmotic stress effects on microbial exoenzyme activities. We also observed a tree-fold increase in the activity of alkaline phosphatases under salinity. This is in line with the threefold increase in available phosphorous that was also observed in the rhizosphere, while a significant correlation between acemannan and P concentration was observed in the *A. vera* leaf rinds under salinity. However, lower alkaline phosphatase activities are generally reported under salinity in soils (Frankenberger and Bingham, 1982; Rietz and Haynes, 2003; Dong et al., 2022). Taken together our results show that in the rhizosphere soil under study potential

microbial enzyme activities were generally sustained and even enhanced under salinity. The soil (typical of a wider area) is loamy sand with only 0.5% organic matter content, and salinity coexists with drought events. We suggest that under these conditions the changes in rhizodeposition and plant root exudation products in the rhizosphere soil environment of the *A. vera* plants may play a key role in sustaining and enhancing substrate induced microbial metabolic activities. The higher availability of Fe in the rhizosphere soil under salinity is in line with changes in root derived C substrates, as they play a major role in enhancing Fe availability in the rhizosphere (Marschner and Römheld, 1994) and phytosiderophore exudation has been specifically shown to increase under salinity (Daneshbakhsh et al., 2013).

4.3 Relationships between plant nutrition, acemannan accumulation and changes in the prokaryoric and fungal communities

Interestingly, the prokaryotic communities in the rhizosphere and the communities of fungi in the roots co-varied with the configuration of the plant responses to salinity. This may just reflect independent effects of salinity, on the assembly of the rhizospheric prokaryotic and root fungal communities and on the accumulation of both Na and acemannan in the leaf gel. Possibly, however, these findings indicate a link of acemannan and Na accumulation *in planta* to prokaryote shifts in the rhizospheres and to fungal shifts in the roots *via* niche specialization and resource acquisition. Prokaryotic microorganisms secrete a plethora of biomolecules (like organic acids and chelators) that profoundly impact solubilization and mobilization of soil nutrients, e.g., phosphorus, potassium, and micronutrients in the rhizosphers soil (Daneshbakhsh et al., 2013). Their community structure under higher salinity is likely both a direct response to, and a driver of, altered ion availabilities which in turn influences the plant's ion uptake and osmotic adjustment, affecting acemannan biosynthesis. Respectively, fungal mycelium networks that colonize plant roots and extend extra-radically improve plant water uptake and modulate nutrient acquisition particularly under salinity stress (Jaiswal et al., 2022). The enrichment in Dark Septate Endophytes (DSE) in rhizophere and erndoroot tissues under high salinity, especially of Papulaspora that include many members know to assist plant to alleviate salinity induced stress supports this view. However, further research and specifically controlled experimentation is needed to validate this hypothesis.

5 Conclusions

This field study revealed coordinated shifts in plant biochemistry and root-associated microbial communities in response to naturally occurring soil salinity gradients in *Aloe vera* cultivation. Under high salinity conditions plants accumulated elevated sodium in leaf gel tissue (2.5-fold increase) alongside increased acemannan content (1.4-fold increase), without apparent impacts on vegetative growth. Our results suggest that *A. vera* plants and their root-associated microbial communities may develop linked responses against salinity as the magnitude of community shifts correlated with the extent of acemannan accumulation and sodium uptake *in planta*. We specifically show characteristic shifts from prokaryotic diderms towards monoderns in the roots of the *A. vera* plants. Our results highlight the importance of joined management of plants and associated microbial communities, to exploit the potential of drought tolerant plants, and optimize their adaptation at an ecosystem level to soil salinity.

Electronic supplementary material

Supplementary material is available in the online version of this article at https://doi.org/10.1007/s42832-026-0409-4 and is accessible for authorized users.

Acknowledgements

The authors sincerely thank *Aloe vera* producers Artemios Chatziartemiou and Dimitrios Liaros, as well as Georgia Mitropoulou, for their invaluable guidance and support. They also extend their gratitude to George Leventis for his technical assistance. Open access funding provided by HEAL-Link Greece.

Author contributions

All authors contributed to the study conception and design. Material preparation, data collection and analysis were performed by Christina Nikolaou and Myrto Tsiknia. The first draft of the manuscript was written by Christina Nikolaou and all authors commented on previous versions of the manuscript. All authors read and approved of the final manuscript.

Data availability

The sequencing data were submitted to Sequence Read Archive of NCBI with BioProject accession number (ID: PRJNA1238781).

Competing interests

The authors declare no competing financial interests.

Open Access

This article is licensed under a Creative Commons Attribution

4.0 International License, which permits use, sharing, adaptation, distribution and reproduction in any medium or format, as long as you give appropriate credit to the original author(s) and the source, provide a link to the Creative Commons licence, and indicate if changes were made. The images or other third party material in this article are included in the article's Creative Commons licence, unless indicated otherwise in a credit line to the material. If material is not included in the article's Creative Commons licence and your intended use is not permitted by statutory regulation or exceeds the permitted use, you will need to obtain permission directly from the copyright holder. To view a copy of this licence, visit http://creativecommons.org/licenses/by/4.0/.

References

Ahl, L.I., Al-Husseini, N., Al-Helle, S., Staerk, D., Grace, O.M., Willats, W.G.T., Mravec, J., Jørgensen, B., Rønsted, N., 2019. Detection of seasonal variation in aloe polysaccharides using carbohydrate detecting microarrays. Frontiers in Plant Science 10, 512.

Akinsanya, M.A., Goh, J.K., Lim, S.P., Ting, A.S.Y., 2015. Metagenomics study of endophytic bacteria in *Aloe vera* using next-generation technology. Genomics Data 6, 159–163.

Ali, A., Maggio, A., Bressan, R.A., Yun, D.J., 2019. Role and functional differences of HKT1-type transporters in plants under salt stress. International Journal of Molecular Sciences 20, 1059.

Ashworth, J., Keyes, D., Kirk, R., Lessard, R., 2001. Standard procedure in the hydrometer method for particle size analysis. Communications in Soil Science and Plant Analysis 32, 633–642.

Assaha, D.V.M., Ueda, A., Saneoka, H., Al-Yahyai, R., Yaish, M.W., 2017. The role of Na^+ and K^+ transporters in salt stress adaptation in glycophytes. Frontiers in Physiology 8, 509.

Bai, Y.J., Niu, Y.M., Qin, S.A., Ma, G.W., 2023. A new biomaterial derived from *Aloe vera*—acemannan from basic studies to clinical application. Pharmaceutics 15, 1913.

Barnard, R.L., Osborne, C.A., Firestone, M.K., 2013. Responses of soil bacterial and fungal communities to extreme desiccation and rewetting. The ISME Journal 7, 2229–2241.

Bekris, F., Vasileiadis, S., Papadopoulou, E., Samaras, A., Testempasis, S., Gkizi, D., Tavlaki, G., Tzima, A., Paplomatas, E., Markakis, E., Karaoglanidis, G., Papadopoulou, K.K., Karpouzas, D.G., 2021. Grapevine wood microbiome analysis identifies key fungal pathogens and potential interactions with the bacterial community implicated in grapevine trunk disease appearance. Environmental Microbiome 16, 23.

Boyrahmadi, M., Raiesi, F., 2018. Plant roots and species moderate the salinity effect on microbial respiration, biomass, and enzyme activities in a sandy clay soil. Biology and Fertility of Soils 54, 509–521.

Breitkreuz, C., Herzig, L., Buscot, F., Reitz, T., Tarkka, M., 2021. Interactions between soil properties, agricultural management and cultivar type drive structural and functional adaptations of the wheat rhizosphere microbiome to drought. Environmental Microbiology 23, 5866–5882.

Bremner, J.M., 1965. Total nitrogen. In: Methods of Soil Analysis. Madison: American Society of Agronomy Inc., 1149–1178.

Bulgarelli, D., Rott, M., Schlaeppi, K., Ver Loren van Themaat, E., Ahmadinejad, N., Assenza, F., Rauf, P., Huettel, B., Reinhardt, R., Schmelzer, E., Peplies, J., Gloeckner, F.O., Amann, R., Eickhorst, T., Schulze-Lefert, P., 2012. Revealing structure and assembly cues for *Arabidopsis* root-inhabiting bacterial microbiota. Nature 488, 91–95.

Callahan, B.J., McMurdie, P.J., Rosen, M.J., Han, A.W., Johnson, A.J.A., Holmes, S.P., 2016. DADA2: high-resolution sample inference from Illumina amplicon data. Nature Methods 13, 581–583.

Caporaso, J.G., Ackermann, G., Apprill, A., Bauer, M., Berg-Lyons, D., Betley, J., Fierer, N., Fraser, L., Fuhrman, J.A., Gilbert, J.A., Gormley, N., Humphrey, G., Huntley, J., Jansson, J.K., Knight, R., Lauber, C.L., Lozupone, C.A., McNally, S., Needham, D.M., Owens, S.M., Parada, A.E., Parsons, R., Smith, G., Thompson, L.R., Thompson, L., Turnbaugh, P.J., Walters, W.A., Weber, L., 2018. EMP 16S Illumina amplicon protocol. Available at the website of protocols.io.

Caporaso, J.G., Lauber, C.L., Walters, W.A., Berg-Lyons, D., Huntley, J., Fierer, N., Owens, S.M., Betley, J., Fraser, L., Bauer, M., Gormley, N., Gilbert, J.A., Smith, G., Knight, R., 2012. Ultra-high-throughput microbial community analysis on the Illumina HiSeq and MiSeq platforms. The ISME Journal 6, 1621–1624.

Cardarelli, M., Rouphael, Y., Rea, E., Lucini, L., Pellizzoni, M., Colla, G., 2013. Effects of fertilization, arbuscular mycorrhiza, and salinity on growth, yield, and bioactive compounds of two *Aloe* species. HortScience 48, 568–575.

Carter, M.R., 1993. Soil Sampling and Methods of Analysis. Boca Raton: Lewis Publishers.

Chen, H.H., Ma, K.Y., Huang, Y., Fu, Q., Qiu, Y.B., Yao, Z.Y., 2022. Significant response of microbial community to increased salinity across wetland ecosystems. Geoderma 415, 115778.

Choi, S.W., Son, B.W., Son, Y.S., Park, Y.I., Lee, S.K., Chung, M.H., 2001. The wound-healing effect of a glycoprotein fraction isolated from aloe vera. British Journal of Dermatology 145, 535–545.

Chowdhury, N., Marschner, P., Burns, R., 2011. Response of microbial activity and community structure to decreasing soil osmotic and matric potential. Plant and Soil 344, 241–254.

Comas-Serra, F., Miró, J.L., Umaña, M.M., Minjares-Fuentes, R., Femenia, A., Mota-Ituarte, M., Pedroza-Sandoval, A., 2024. Role of acemannan and pectic polysaccharides in saline-water stress tolerance of *Aloe vera* (*Aloe barbadensis* Miller) plant. International Journal of Biological Macromolecules 268, 131601.

Connell, J.H., 1978. Diversity in tropical rain forests and coral reefs: high diversity of trees and corals is maintained only in a nonequilibrium state. Science 199, 1302–1310.

Daneshbakhsh, B., Khoshgoftarmanesh, A.H., Shariatmadari, H., Cakmak, I., 2013. Phytosiderophore release by wheat genotypes differing in zinc deficiency tolerance grown with Zn-free nutrient solution as affected by salinity. Journal of Plant Physiology 170, 41–46.

Deinlein, U., Stephan, A.B., Horie, T., Luo, W., Xu, G.H., Schroeder, J.I., 2014. Plant salt-tolerance mechanisms. Trends in Plant Science 19, 371–379.

Derouiche, M., Mzabri, I., Ouahhoud, S., Dehmani, I., Benabess, R., Addi, M., Hano, C., Boukroute, A., Berrichi, A., Kouddane, N., 2023. The effect of salt stress on the growth and development of three *Aloe* species in eastern Morocco. Plant Stress 9, 100187.

Dilukshi Fernando, V.C., Schroeder, D.F., 2016. Role of ABA in Arabidopsis salt, drought, and desiccation tolerance. In: Shanker, A.K., Shanker, C., eds. Abiotic and Biotic Stress in Plants - Recent Advances and Future Perspectives. Rijeka: InTech.

Dixon, P., 2003. VEGAN, a package of R functions for community ecology. Journal of Vegetation Science 14, 927–930.

Dodt, M., Roehr, J.T., Ahmed, R., Dieterich, C., 2012. FLEXBAR-flexible barcode and adapter processing for next-generation sequencing platforms. Biology 1, 895–905.

Dong, Y., Chen, R., Petropoulos, E., Yu, B., Zhang, J., Lin, X., Gao, M., Feng, Y., 2022. Interactive effects of salinity and SOM on the ecoenzymatic activities across coastal soils subjected to a saline gradient. Geoderma 406, 115519.

Eberendu, A.R., Luta, G., Edwards, J.A., McAnalley, B.H., Davis, B., Rodriguez, S., Ray Henry, C., 2005. Quantitative colorimetric analysis of aloe polysaccharides as a measure of *Aloe vera* quality in commercial products. Journal of AOAC INTERNATIONAL 88, 684–691.

FAO, 2020. Soil Testing Methods Manual. Rome: FAO.

Femenia, A., Sánchez, E.S., Simal, S., Rosselló, C., 1999. Compositional features of polysaccharides from Aloe vera (*Aloe barbadensis* Miller) plant tissues. Carbohydrate Polymers 39, 109–117.

Fradera-Soler, M., Grace, O.M., Jørgensen, B., Mravec, J., 2022. Elastic and collapsible: current understanding of cell walls in succulent plants. Journal of Experimental Botany 73, 2290–2307.

Frankenberger, W.T.Jr., Bingham, F.T., 1982. Influence of salinity on soil enzyme activities. Soil Science Society of America Journal 46, 1173–1177.

Furze, J.R., Martin, A.R., Nasielski, J., Thevathasan, N.V., Gordon, A.M., Isaac, M.E., 2017. Resistance and resilience of root fungal communities to water limitation in a temperate agroecosystem. Ecology and Evolution 7, 3443–3454.

González-Delgado, M., Minjares-Fuentes, R., Mota-Ituarte, M., Pedroza-Sandoval, A., Comas-Serra, F., Quezada-Rivera, J.J., Sáenz-Esqueda, Á., Femenia, A., 2023. Joint water and salinity stresses increase the bioactive compounds of *Aloe vera* (*Aloe barbadensis* Miller) gel enhancing its related functional properties. Agricultural Water Management 285, 108374.

Grime, J.P., 1973. Competitive exclusion in herbaceous vegetation. Nature 242, 344–347.

Ihrmark, K., Bödeker, I.T.M., Cruz-Martinez, K., Friberg, H., Kubartova, A., Schenck, J., Strid, Y., Stenlid, J., Brandström-Durling, M., Clemmensen, K.E., Lindahl, B.D., 2012. New primers to amplify the fungal ITS2 region-evaluation by 454-sequencing of artificial and natural communities. FEMS Microbiology Ecology 82, 666–677.

Jackson, C.R., Tyler, H.L., Millar, J.J., 2013. Determination of microbial extracellular enzyme activity in waters, soils, and sediments using high throughput microplate assays. Journal of Visualized Experiments, e50399.

Jaiswal, L.K., Singh, P., Singh, R.K., Nayak, T., Tripathi, Y.N., Upadhyay, R.S., Gupta, A., 2022. Effects of salt stress on nutrient cycle and uptake of crop plants. In: Singh, P., Singh, M., Singh, R.K., Prasad, S.M., eds. Physiology of Salt Stress in Plants. Hoboken: John Wiley & Sons Ltd., 129–153.

Jales, S.T.L., de Melo Barbosa, R., da Silva, G.R., Severino, P., de Lima Moura, T.F.A., 2021. Natural polysaccharides from *Aloe vera* L. gel (*Aloe barbadensis* miller): processing techniques and analytical methods, In: Inamuddin, Ahamed, M.I., Boddula, R., Altalhi, T., eds. Polysaccharides. Hoboken: Wiley, 1–22.

Jian, S.Y., Li, J.W., Chen, J., Wang, G.S., Mayes, M.A., Dzantor, K.E., Hui, D.F., Luo, Y.O., 2016. Soil extracellular enzyme activities, soil carbon and nitrogen storage under nitrogen fertilization: a meta-analysis. Soil Biology and Biochemistry 101, 32–43.

Kassambara, A., 2023. ggpubr: “ggplot2” based publication ready plots. Available at the website of rpkgs.datanovia.com/ggpubr/.

Knight, H., Trewavas, A.J., Knight, M.R., 1997. Calcium signalling in *Arabidopsis thaliana* responding to drought and salinity. The Plant Journal 12, 1067–1078.

Koyama, A., Steinweg, J.M., Haddix, M.L., Dukes, J.S., Wallenstein, M.D., 2018. Soil bacterial community responses to altered precipitation and temperature regimes in an old field grassland are mediated by plants. FEMS Microbiology Ecology 94, fix156.

Lindsay, W.L., Norvell, W.A., 1978. Development of a DTPA soil test for zinc, iron, manganese, and copper. Soil Science Society of America Journal 42, 421–428.

Litalien, A., Zeeb, B., 2020. Curing the earth: a review of anthropogenic soil salinization and plant-based strategies for sustainable mitigation. Science of the Total Environment 698, 134235.

Liu, C., Cui, Y.M., Li, X.Z., Yao, M.J., 2021. *microeco*: an R package for data mining in microbial community ecology. FEMS Microbiology Ecology 97, fiaa255.

Mai-Prochnow, A., Clauson, M., Hong, J., Murphy, A.B., 2016. Gram positive and Gram negative bacteria differ in their sensitivity to cold plasma. Scientific Reports 6, 38610.

Mandyam, K., Jumpponen, A., 2005. Seeking the elusive function of the root-colonising dark septate endophytic fungi. Studies in Mycology 53, 173–189.

Marschner, H., Römheld, V., 1994. Strategies of plants for acquisition of iron. Plant and Soil 165, 261–274.

Morrissey, E.M., Gillespie, J.L., Morina, J.C., Franklin, R.B., 2014. Salinity affects microbial activity and soil organic matter content in tidal wetlands. Global Change Biology 20, 1351–1362.

Munns, R., Tester, M., 2008. Mechanisms of salinity tolerance. Annual Review of Plant Biology 59, 651–681.

Nakkeeran, S., Rajamanickam, S., Saravanan, R., Vanthana, M., Soorianathasundaram, K., 2021. Bacterial endophytome-mediated resistance in banana for the management of *Fusarium* wilt. 3 Biotech 11, 267.

Nelson, D.R., Mele, P.M., 2007. Subtle changes in rhizosphere microbial community structure in response to increased boron and sodium chloride concentrations. Soil Biology and Biochemistry 39, 340–351.

Nelson, D.W., Sommers, L.E., 1996. Total carbon, organic carbon, and organic matter. In: Sparks, D.L., Page, A.L., Helmke, P.A.,

Loeppert, R.H., Soltanpour, P.N., Tabatabai, M.A., Johnston, C.T., Sumner, M.E., eds. Methods of Soil Analysis. Madison: Soil Science Society of America, 539–579.

Nikolaou, C.N., Chatziartemiou, A., Tsiknia, M., Karyda, A.G., Ehaliotis, C., Gasparatos, D., 2023. Calcium- and magnesium-enriched organic fertilizer and plant growth-promoting rhizobacteria affect soil nutrient availability, plant nutrient uptake, and secondary metabolite production in *Aloe vera* (*Aloe barbadensis* miller) grown under field conditions. Agronomy 13, 482.

Nilsson, R.H., Larsson, K.H., Taylor, A.F.S., Bengtsson-Palme, J., Jeppesen, T.S., Schigel, D., Kennedy, P., Picard, K., Glöckner, F.O., Tedersoo, L., Saar, I., Kõljalg, U., Abarenkov, K., 2019. The UNITE database for molecular identification of fungi: handling dark taxa and parallel taxonomic classifications. Nucleic Acids Research 47, D259–D264.

Ntanos, E., Kekelis, P., Assimakopoulou, A., Gasparatos, D., Denaxa, N.K., Tsafouros, A., Roussos, P.A., 2021. Amelioration effects against salinity stress in strawberry by bentonite–zeolite mixture, glycine betaine, and *Bacillus amyloliquefaciens* in terms of plant growth, nutrient content, soil properties, yield, and fruit quality characteristics. Applied Sciences 11, 8796.

Olsen, S.R., 1954. Estimation of Available Phosphorus in Soils by Extraction with Sodium Bicarbonate. Washington: United States Department of Agriculture.

Pankhurst, C.E., Yu, S., Hawke, B.G., Harch, B.D., 2001. Capacity of fatty acid profiles and substrate utilization patterns to describe differences in soil microbial communities associated with increased salinity or alkalinity at three locations in South Australia. Biology and Fertility of Soils 33, 204–217.

Parham, J.A., Deng, S.P., 2000. Detection, quantification and characterization of β-glucosaminidase activity in soil. Soil Biology and Biochemistry 32, 1183–1190.

Parks, D.H., Chuvochina, M., Chaumeil, P.A., Rinke, C., Mussig, A.J., Hugenholtz, P., 2020. A complete domain-to-species taxonomy for Bacteria and Archaea. Nature Biotechnology 38, 1079–1086.

Philippot, L., Chenu, C., Kappler, A., Rillig, M.C., Fierer, N., 2024. The interplay between microbial communities and soil properties. Nature Reviews Microbiology 22, 226–239.

Philippot, L., Griffiths, B.S., Langenheder, S., 2021. Microbial community resilience across ecosystems and multiple disturbances. Microbiology and Molecular Biology Reviews 85, e00026–20.

Quast, C., Pruesse, E., Yilmaz, P., Gerken, J., Schweer, T., Yarza, P., Peplies, J., Glöckner, F.O., 2013. The SILVA ribosomal RNA gene database project: improved data processing and web-based tools. Nucleic Acids Research 41, D590–596.

Quezada, M.P., Salinas, C., Gotteland, M., Cardemil, L., 2017. Acemannan and fructans from aloe vera (*Aloe barbadensis* miller) plants as novel prebiotics. Journal of Agricultural and Food Chemistry 65, 10029–10039.

Rath, K.M., Rousk, J., 2015. Salt effects on the soil microbial decomposer community and their role in organic carbon cycling: a review. Soil Biology and Biochemistry 81, 108–123.

Rietz, D.N., Haynes, R.J., 2003. Effects of irrigation-induced salinity and sodicity on soil microbial activity. Soil Biology and Biochemistry 35, 845–854.

Roberts, S.K., Snowman, B.N., 2000. The effects of ABA on channel-mediated K^+ transport across higher plant roots. Journal of Experimental Botany 51, 1585–1594.

Roussos, P.A., Gasparatos, D., Kyriakou, C., Tsichli, K., Tsantili, E., Haidouti, C., 2013. Growth, nutrient status, and biochemical changes of sour orange plants subjected to sodium chloride stress. Communications in Soil Science and Plant Analysis 44, 805–816.

Salinas, P., Salinas, C., Contreras, R.A., Zuñiga, G.E., Dupree, P., Cardemil, L., 2019. Water deficit and abscisic acid treatments increase the expression of a glucomannan mannosyltransferase gene (*GMMT*) in *Aloe vera* Burm. F. Phytochemistry 159, 90–101.

Santos-Medellín, C., Edwards, J., Liechty, Z., Nguyen, B., Sundaresan, V., 2017. Drought stress results in a compartment-specific restructuring of the rice root-associated microbiomes. mBio 8, e00764–17.

Shabala, S., Pottosin, I., 2014. Regulation of potassium transport in plants under hostile conditions: implications for abiotic and biotic stress tolerance. Physiologia Plantarum 151, 257–279.

Shanker, A., Venkateswarlu, B., 2011. Abiotic Stress in Plants-Mechanisms and Adaptations. Rijeka: InTechOpen.

Singh, K., 2016. Microbial and enzyme activities of saline and sodic soils. Land Degradation & Development 27, 706–718.

Sinsabaugh, R.L., Lauber, C.L., Weintraub, M.N., Ahmed, B., Allison, S.D., Crenshaw, C., Contosta, A.R., Cusack, D., Frey, S., Gallo, M.E., Gartner, T.B., Hobbie, S.E., Holland, K., Keeler, B.L., Powers, J.S., Stursova, M., Takacs-Vesbach, C., Waldrop, M.P., Wallenstein, M.D., Zak, D.R., Zeglin, L.H., 2008. Stoichiometry of soil enzyme activity at global scale. Ecology Letters 11, 1252–1264.

Sultana, T., Chowdhury, A.H., Saha, B.K., Rahman, A., Chowdhury, T., Sultana, R., 2021. Response of *Aloe vera* to potassium fertilization in relation to leaf biomass yield, its uptake and requirement, critical concentration and use efficiency. Journal of Plant Nutrition 44, 2081–2095.

Sun, D.S., Li, K.J., Bi, Q.F., Zhu, J., Zhang, Q.C., Jin, C.W., Lu, L.L., Lin, X.Y., 2017. Effects of organic amendment on soil aggregation and microbial community composition during drying-rewetting alternation. Science of the Total Environment 574, 735–743.

Tabatabai, M.A., 1994. Soil enzymes. In: Black, C.A., ed. Methods of Soil Analysis. Madison: The American Society of Agronomy, 775–833.

Tester, M., Davenport, R., 2003. Na^+ tolerance and Na^+ transport in higher plants. Annals of Botany 91, 503–527.

van Zelm, E., Zhang, Y.X., Testerink, C., 2020. Salt tolerance mechanisms of plants. Annual Review of Plant Biology 71, 403–433.

Vasileiadis, S., Puglisi, E., Papadopoulou, E.S., Pertile, G., Suciu, N., Pappolla, R.A., Tourna, M., Karas, P.A., Papadimitriou, F., Kasiotakis, A., Ipsilanti, N., Ferrarini, A., Sułowicz, S., Fornasier, F., Menkissoglu-Spiroudi, U., Nicol, G.W., Trevisan, M., Karpouzas, D.G., 2018. Blame it on the metabolite: 3,5-dichloroaniline rather than the parent compound is responsible for the decreasing diversity and function of soil microorganisms. Applied

and Environmental Microbiology 84, e01536–18.

Vasileiadis, S., Puglisi, E., Trevisan, M., Scheckel, K.G., Langdon, K.A., McLaughlin, M.J., Lombi, E., Donner, E., 2015. Changes in soil bacterial communities and diversity in response to long-term silver exposure. FEMS Microbiology Ecology 91, fiv114.

Walters, W., Hyde, E.R., Berg-Lyons, D., Ackermann, G., Humphrey, G., Parada, A., Gilbert, J.A., Jansson, J.K., Caporaso, J.G., Fuhrman, J.A., Apprill, A., Knight, R., 2016. Improved bacterial 16S rRNA gene (V4 and V4-5) and fungal internal transcribed spacer marker gene primers for microbial community surveys. mSystems 1, e00009–15.

Wang, W., Vinocur, B., Altman, A., 2003. Plant responses to drought, salinity and extreme temperatures: towards genetic engineering for stress tolerance. Planta 218, 1–14.

White, D.C., Sutton, S.D., Ringelberg, D.B., 1996. The genus *Sphingomonas*: physiology and ecology. Current Opinion in Biotechnology 7, 301–306.

Wichern, J., Wichern, F., Joergensen, R.G., 2006. Impact of salinity on soil microbial communities and the decomposition of maize in acidic soils. Geoderma 137, 100–108.

Wickham, H., 2016. Getting Started with ggplot2. In: Wickham, H., ed. ggplot2: Elegant Graphics for Data Analysis. Cham: Springer, 11–31.

Xu, J.S., Gao, W., Zhao, B.Z., Chen, M.Q., Ma, L., Jia, Z.J., Zhang, J.B., 2021. Bacterial community composition and assembly along a natural sodicity/salinity gradient in surface and subsurface soils. Applied Soil Ecology 157, 103731.

Xu, L., Coleman-Derr, D., 2019. Causes and consequences of a conserved bacterial root microbiome response to drought stress. Current Opinion in Microbiology 49, 1–6.

Xu, L., Naylor, D., Dong, Z.B., Simmons, T., Pierroz, G., Hixson, K.K., Kim, Y.M., Zink, E.M., Engbrecht, K.M., Wang, Y., Gao, C., DeGraaf, S., Madera, M.A., Sievert, J.A., Hollingsworth, J., Birdseye, D., Scheller, H.V., Hutmacher, R., Dahlberg, J., Jansson, C., Taylor, J.W., Lemaux, P.G., Coleman-Derr, D., 2018. Drought delays development of the sorghum root microbiome and enriches for monoderm bacteria. Proceedings of the National Academy of Sciences of the United States of America 115, E4284–E4293.

Yilmaz, P., Parfrey, L.W., Yarza, P., Gerken, J., Pruesse, E., Quast, C., Schweer, T., Peplies, J., Ludwig, W., Glöckner, F.O., 2014. The SILVA and "All-species Living Tree Project (LTP)" taxonomic frameworks. Nucleic Acids Research 42, D643–D648.

Yuan, Z.L., Druzhinina, I.S., Labbé, J., Redman, R., Qin, Y., Rodriguez, R., Zhang, C.L., Tuskan, G.A., Lin, F.C., 2016. Specialized microbiome of a halophyte and its role in helping non-host plants to withstand salinity. Scientific Reports 6, 32467.

Zhang, G.L., Bai, J.H., Jia, J., Wang, W., Wang, D.W., Zhao, Q.Q., Wang, C., Chen, G.Z., 2023. Soil microbial communities regulate the threshold effect of salinity stress on SOM decomposition in coastal salt marshes. Fundamental Research 3, 868–879.

Zhang, X.M., Johnston, E.R., Barberán, A., Ren, Y., Wang, Z.P., Han, X.G., 2018. Effect of intermediate disturbance on soil microbial functional diversity depends on the amount of effective resources. Environmental Microbiology 20, 3862–3875.

Zheljazkov, V.D., Warman, P.R., 2002. Comparison of three digestion methods for the recovery of 17 plant essential nutrients and trace elements from six composts. Compost Science & Utilization 10, 197–203.

Zhou, H.P., Shi, H.F., Yang, Y.Q., Feng, X.X., Chen, X., Xiao, F., Lin, H.H., Guo, Y., 2024. Insights into plant salt stress signaling and tolerance. Journal of Genetics and Genomics 51, 16–34.

Zhou, M.H., Butterbach-Bahl, K., Vereecken, H., Brüggemann, N., 2017. A meta-analysis of soil salinization effects on nitrogen pools, cycles and fluxes in coastal ecosystems. Global Change Biology 23, 1338–1352.